Environmental Science and Pollution Research (2020) 27:29502–29511
https://doi.org/10.1007/s11356-020-09122-3

RESEARCH ARTICLE

Annual study of hydraulic characteristics in surface flow constructed wetlands using hydrogen and oxygen stable isotope technology

Hang Gao[1] · Wei Lan[1] · Haimeng Sun[1,2] · Zhen Hu[1]

Received: 22 November 2019 / Accepted: 29 April 2020 / Published online: 22 May 2020

Abstract

Complex flow patterns and hydraulic characteristics could reduce the utilization efficiency of constructed wetland (CW), and consequently, its pollutant removal performance. Thus, it is of great importance to explore the internal flow patterns of CWs. Isotopic molecules exist naturally in CWs and have special properties under liquid conditions; using hydrogen and oxygen isotope technology cannot only reduce secondary pollution but also reflect the hydraulic characteristics of CWs. In the present study, the annual variation of isotopic composition in field-scale CW was investigated to evaluate the long-term feasibility of stable isotopic technology characterizing hydraulic flow patterns. The relationship between nutrients concentration distribution and flow pattern variation in CW under different seasons was discussed as well. Results demonstrated that isotope $^{18}O/^{16}O$ distribution could be used to determine the internal flow pattern of CW throughout the year, except for preferential flow area of CWs in winter, since more hydraulic retention time is needed to ensure the change of water isotopes due to the small evaporation in winter. Lower ammonia nitrogen concentration was observed in the stagnant area, while the total phosphorus concentration of the stagnant area increased during winter. And more attention should be paid to aquatic plants during the CW design, since it has significant influence on the hydraulic flow patterns of CW.

Keyword Constructed wetland · Hydraulic flow patterns · Water isotopes · Ammonia · Total phosphorus · Evaporation

Introduction

Constructed wetland (CW), which was composed of substrate, aquatic plants, animals and microorganisms, has been recognized as an ecological technology for wastewater treatment (Vymazal 2010). It has been designed and constructed to purify domestic sewage, urban runoff, and industrial effluents worldwide in the last few decades (Vymazal 2011). Generally, the removal of nutrients mainly depends on sedimentation and adsorption by media, plant uptake, and various microbial process such as nitrification and denitrification (Vymazal 2007). Compared to other conventional sewage treatment processes, CW has its advantages of low energy requirement, stable operation, and simple maintenance.

However, the internal flow pattern and hydrodynamic behavior in different areas of CWs were diverse. There were even some stagnant zones, short-circuiting flow zones, and preferential flow areas leading to the decline of removal efficiencies due to the regional differences of plant species and density, as well as flow passage shape in CW (Sun et al. 2016). Therefore, it was of great importance to investigate the flow pattern and hydraulic characteristics in different areas of CW, to improve its contaminant removal efficiencies (Tang et al. 2017).

At present, many researchers focused on the application of velocity measurement, mathematical models, or tracer to simulate hydraulic flow patterns in CW. Velocity measurement technology based on acoustic Doppler velocimeters (ADVs) has revolutionized the measurement of mean velocities, the flow characteristics, and turbulence parameters in laboratory and field researches in the early 1990s (Muste et al. 2007). This technology was firstly adopted in the field of riverine studies in terms of velocity measurement broadly (Nyantekyi-Kwakye et al. 2017). Das and Mazumdar (2015)

Hang Gao and Wei Lan contributed equally to this work.

Responsible editor: Philippe Garrigues

✉ Zhen Hu
huzhen885@sdu.edu.cn

1 Shandong Key Laboratory of Water Pollution Control and Resource Reuse, School of Environmental Science & Engineering, Shandong University, Qingdao 266237, China

2 Department of Environmental Science, College of Environmental Sciences & Engineering, Peking University, Beijing 100871, China

used the velocity vector measured by ADVs to deduce the contours and spatial distributions of the time-averaged velocities and turbulence intensities. However, direct velocity measurement in field-scale CW was known as a high-cost and labor-consuming job.

On the other hand, several mathematical models, such as Water Quality Analysis Simulation Program, Surface Water Modeling System, and MIKE (Model-based and Incremental Knowledge), have been introduced as tools to obtain a deep understanding of hydraulic characteristics of CW (Qi et al. 2013). In the previous study, the influence of topographic and plant on the formation of short-circuiting flow zones in CW was estimated by the simulation model MIKE 21 (Min and Wise 2009).

Yet the results obtained by the mathematical model could not reflect the hydraulic flow patterns synchronously because its parameters were mostly empirical. This is why tracer method, which has an advantage of ignoring information of fluid properties before measurement (Lin et al. 2003), was currently widely used to determine the hydraulic flow patterns in CW (Guo et al. 2017; Pugliese et al. 2020; Bodin et al. 2012; Plugatyr and Svishchev 2008). The hydraulic behavior includes residence time distribution and the effective volume ratio in three full-scale surface flow constructed wetlands (SFCWs) were investigated by multi-tracer involving uranine and sulforhodamine B. Residence time distribution analysis shows that the three investigated wetlands displayed very different hydrodynamic properties (Laurent et al. 2015; Liu et al. 2020). However, in large-scale CWs, adding tracers was not a good choice because of the high cost and the potential of secondary pollution induced by external additives. More importantly, the tracer method could not provide information on the location of stagnant zones and short-circuiting flow areas inside CW. Hence, an alternative method should be developed to address these prominent problems (Zheng et al. 2011).

In recent years, more and more attention has been paid to the usage of stable isotope, e.g., hydrogen and oxygen isotopes, to predict the hydraulic characteristics of CW (Bugna et al. 2020). Under the liquid condition, the vapor pressure of isotopic molecule is inversely proportional to its molecular weight, which led to the enrichment of heavy isotopes involving ^{2}H and ^{18}O (Ronkanen and Klove 2007). The abundance of heavy water isotopes ($\delta^{2}H$ and $\delta^{18}O$ values) therefore would be elevated in stagnant or dead zones with a longer hydraulic retention time (HRT). Compared with conventional methods, the stable hydrogen and oxygen isotopes are more cost-effective and environmental friendly, reflect the on-site conditions of the hydraulic characteristics of CWs. In the previous study, Ronkanen and Klove (2007) indicated that the stable isotope method enables an accurate evaluation of the flow patterns in natural peatlands on the basis of $^{18}O/^{16}O$ distribution. It is commonly known that vapor pressure increased with temperature; however, to date, annual study on using stable isotope in CW is still lacking.

Herein, the main objectives of this study were as follows: (1) to assess the long-term feasibility of the stable isotope method for determining hydraulic flow patterns in CW; (2) to evaluate how important role the inflow and outflow types and aquatic plant played in hydraulic flow patterns of CW; (3) to explore the correlation between hydraulic characteristics and contaminants removal of CW.

Materials and methods

Study area description

In this study, two surface flow CWs, namely Xiaomei river CW and Tuhai river CW, were selected as the research objects. Effluent from local wastewater treatment plants (WWTPs) dominated pollutant loads (N, P) discharged into both CWs.

Xiaomei river CW, with an area of 1.4 ha and the water treatment capacity of 20,000 m^3/day, was constructed along the watercourse of Xiaomei river located in Liaocheng (115° 16′ ~ 116° 32′ E, 35° 47′ ~ 37° 02′ N), Shandong Province. Geographically, Liaocheng is dominated by the warm temperate continental monsoon climate, which has an annual mean precipitation of 602.5 mm, an annual mean temperature of 13.1 °C, and an annual mean relative humidity of 62%. Wastewater flows into the CW through water distribution ditch and then discharged into Xiaomei river with the outflow type of unilateral overflow. The surface flow area of Xiaomei river CW, which is planted with *Phragmites*, *Lotos*, and *Crispus*, has an irregular pentagon shape and the designed water depth is 0.5 m.

Tuhai river CW is the combination of subsurface flow CW and surface flow CW, with the water treatment capacity of 30,000 m^3/day. Its total area is 2.1 ha and is located in Yucheng of Dezhou (116° 22′ ~ 116° 45′ E, 35° 41′ ~ 37° 12′ N), Shandong Province. The climate of Yucheng is similar to that in Liaocheng, with an annual mean precipitation of 555.5 mm, annual mean temperature of 13.3 °C, and an annual mean relative humidity of 65%. Inlet and outflow of this CW are equipped with over-fall weirs. The surface flow area of Tuhai river CW are planted with emergent vegetation (*Zizania aquatica*); the average design water depth is 0.7 m and has an irregular shape. The detailed information on hydraulic parameters of both CWs is shown in Table 1.

Sampling

We set up three vertical lines and divided each vertical line equally. Then, five sampling points are established uniformly in each vertical line. Each point is spaced approximately 20 m apart (SEPA 2002). Water samples in Xiaomei river CW were collected seasonally in April, July, October, and December of

Table 1 The information on hydraulic parameters in experimental CWs

Wetlands	Parameters							
	Area (ha)	Water treatment capacity(m^3 day^{-1})	Flow rate (m^3 day^{-1})	Influent modes	Effluent modes	The sharp of water flows	Plant types	Plant density
Xiaomei river CW	1.4	20,000	2.0×10^4	Water distribution ditch	Outlet ditch	Irregular pentagon	Emergent and submerged plants	35 plants m^{-2}
Tuhai river CW	2.1	30,000	3.0×10^4	Over-fall weirs	Over-fall weirs	Irregular	Emergent plants	55 plants m^{-2}

2017, while the samples of Tuhai river CW were collected in identical months of 2017, respectively. For each sampling point, three parallel water samples were collected 10 cm below water level, under the specific condition that is windless and no precipitation for ten consecutive days or more. Collected water samples were stored in an icebox using 50-mL polyethylene bottles, subsequently transported to the laboratory and kept in a freezer with a controlled temperature of − 4 °C for the following analyses. The software of Google Earth and GPS (629sc, Garmin, Taiwan, China) were employed in this study to determine the detailed geographic location of all sampling points, such as latitude and longitude. The sampling points and wetland shapes are shown in Fig. 1.

Principles and analysis

Among the various elements in nature, the number of atoms is the determining factor in the chemical properties of the various elements. Therefore, there is almost no difference in chemical properties between various isotopes with the same atomic number. However, due to the different number of neutrons, the mass of each isotope is different. The difference in mass causes the isotope fractionation phenomenon (Lécuyer et al. 2013). Phase change is the main factor that causes isotope sharing, such as evaporation of water, condensation of rain, snow, and melting. Stable isotopes in different regions and different water forms have regular changes. The isotope analyses were conducted by Picarro Isotopic Water Analyzer L2140-I, based on wavelength-scanned cavity ring-down spectroscopy (WS-CRDS) technology (Gupta et al. 2009). $^2H/^1H$ and $^{18}O/^{16}O$ ratios of samples were measured with pre-treatment of 0.45-μm high capacity filter (Gooddy et al. 2016). Results of stable isotope analyses were expressed in delta notation (δ) as part per thousand (‰) deviations versus Vienna Standard Mean Ocean Water (VSMOW). Analytical precision was ± 0.100‰ and ± 0.025‰ for δ^2H and $\delta^{18}O$, respectively (Sun et al. 2016). Water samples for ammonia nitrogen and total phosphorus concentration analyses were filtered by a 0.22-μm filter following the standard photometric method (APHA 2017).

Data analysis

Based on the Kriging method and Surfer 11.0 software, all data, including isotopic composition and pollutant concentration, were processed by the interpolation method to generate distribution maps visually (Woodard 2000).

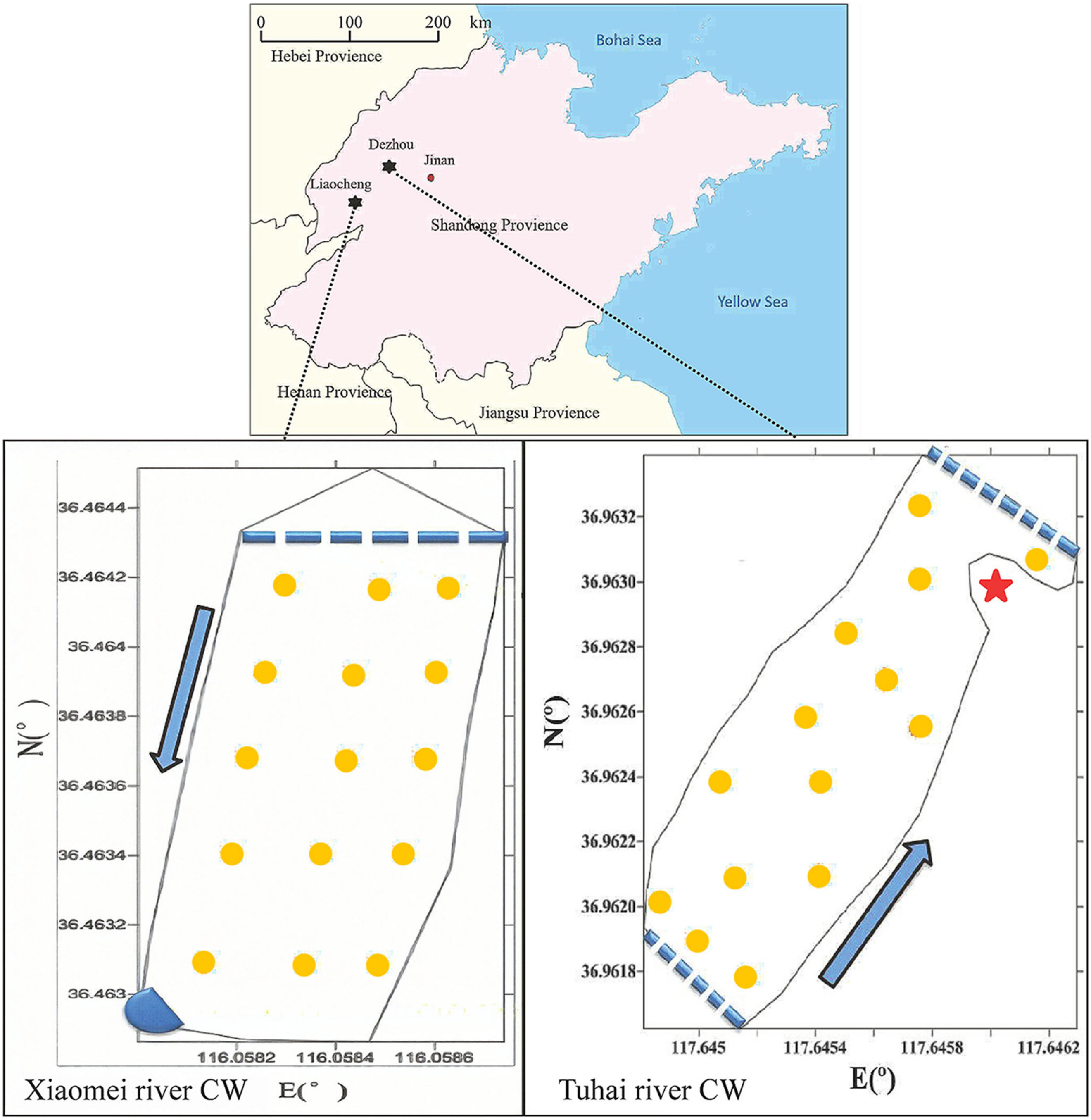

Fig. 1 Geographical location and sampling map of Xiaomei river CW and Tuhai river CW (arrows represent the direction of water flow; orange dots represent sampling points; red pentagram represents artificial island)

Table 2 Annual stable isotope composition of Xiaomei river CW

Season	Mean value (‰)		Range of variation (‰)		Amplitude (‰)	
	δD	$\delta^{18}O$	δD	$\delta^{18}O$	δD	$\delta^{18}O$
Spring	− 57.62	− 7.59	− 59.67 ~ − 52.26	− 7.80 ~ − 6.89	7.40	0.91
Summer	− 56.56	− 7.69	− 59.01 ~ − 52.98	− 7.99 ~ − 7.22	6.03	0.77
Autumn	− 55.67	− 7.57	− 59.07 ~ − 53.72	− 8.01 ~ − 7.27	5.35	0.74
Winter	− 60.75	− 8.24	− 61.88 ~ − 58.21	− 8.34 ~ − 7.89	3.67	0.45

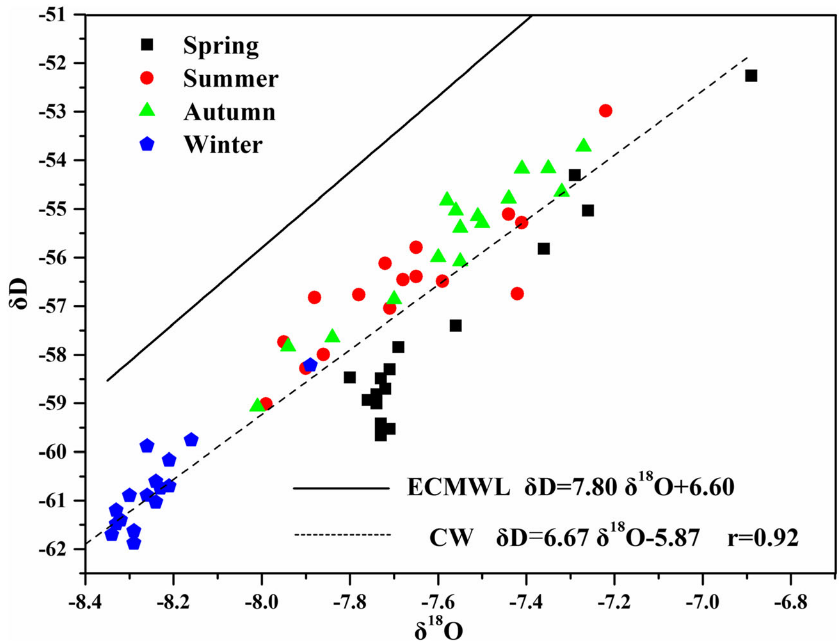

Fig. 2 Relationship between surface water signatures of δD and $\delta^{18}O$ for CW relative to the eastern China meteoric water line (ECMWL)

Results and discussions

Annual feasibility study of stable isotopes

The annual hydrogen and oxygen isotopic compositions of Xiaomei river CW

The annual variation of stable isotope composition in Xiaomei River CW is shown in Table 2. In each season, the difference in stable isotope composition caused by evaporation was observed, indicating the regional difference of hydraulic flow patterns. The correlation relationship between δD and $\delta^{18}O$ in Xiaomei river CW was δD = 6.67 $\delta^{18}O$-5.87 (r = 0.92), with the correlation coefficient of 0.86, as shown in Fig. 2. All stable isotopes dropped to the right side of the eastern China meteoric water line (ECMWL), with the slope and intercept of the fitting line less than that of ECMWL (Yu et al. 1987). This was caused by the strong evaporation in the area where Xiaomei river CW located.

In the winter, δD fluctuated between − 61.88 and − 58.21‰ with the amplitude of 3.67‰, while $\delta^{18}O$ was ranged from − 8.34 to − 7.89‰ with the amplitude of 0.45‰ in Xiaomei river CW. The average values and amplitude variation were all weaker than other seasons, which was caused by the decrease of air temperature and evaporation in winter. This also explained the decreased amplitude variation of isotopic composition (Kele et al. 2011). And interestingly, the mean δD and $\delta^{18}O$ values in summer were − 56.56‰ and − 7.69‰, respectively, similar to that in spring and autumn. Relatively strong evaporation did not lead to a significant increase in average water isotopic compositions, mainly due to the supplement of precipitation during the process of water

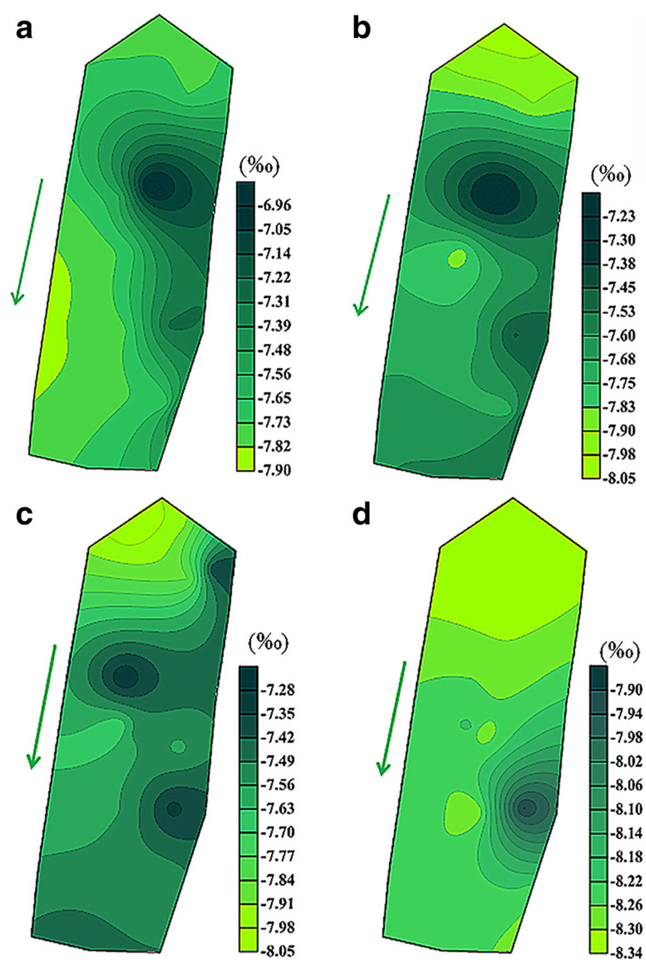

Fig. 3 The $\delta^{18}O$ distribution of Xiaomei river CW in spring (**a**), summer (**b**), autumn (**c**), and winter (**d**). (Arrows represent the direction of water flow)

flow. Dayem et al. (2010) demonstrated that precipitation had a great influence on the isotopic composition of the surface water, and $\delta^{18}O$ values even expressed a fatal decline in rainy season.

Water isotope distribution

The oxygen isotope distribution in Xiaomei river CW during different seasons is shown in Fig. 3. Throughout the year, the region with minimum $\delta^{18}O$ value was located at the inlet of CWs. As the wastewater flowed through CW, $\delta^{18}O$ values raised with the increasing cumulative evaporation. However, the peak value of $\delta^{18}O$ appeared inside the CW, rather than the outlet of CW. To better describe the water flow patterns, dark area with high $\delta^{18}O$ value was regarded as a stagnant area (SA), while the area with sparse contours was defined as preferential flow area (PFA). The stagnant area is the area where the water flow is stagnant for some reason and the water flow speed is slow. The preferential flow is the area where the water flows preferentially for some reason and the area where the water flow is faster.

Figure 3 a showed that SAs ($\delta^{18}O > -7.05‰$) were located at E 116.05849° N 36.46389° and E 116.05858° N 36.46339° in spring, where heavy isotope has a large degree of enrichment. The west side of CWs was considered as PFAs, in which $\delta^{18}O$ values ranged from − 7.82 to − 7.73‰, and the ^{18}O content was closed to the inflow of CW, indicating that evaporation of surface water body in CW was not sufficient and heavy isotope ^{18}O failed to enrich.

In summer, the location of SAs (E 116.05850° N 36.46388° and E 116.05856° N 36.46337°) were well-marked; however, the size of SAs was slightly larger than that in spring. Likewise, the size of PFAs was expanded as well despite weak geographic change. In autumn, the number of SA increased and $\delta^{18}O$ values were higher than − 7.35‰. The location of SAs was E 116.05870° N 36.46425°, E 116.05838° N 36.46386°, and E 116.05857° N 36.46339°, which were in agreement with those in spring and summer. This was possibly caused by the withered aquatic plants in autumn. In addition, the contours of $\delta^{18}O$ values were relatively uniform in autumn and no distinct PFA was determined.

Compared to other seasons, $\delta^{18}O$ values required longer hydraulic retention time to change in winter because of low evaporation. Therefore, it is unqualified to judge whether PFAs present or not in terms of contour distribution of $\delta^{18}O$ values, although one SA (E 116.05855° N 36.46339°) could be determined in Fig. 3d. In conclusion, stable oxygen isotope technology could identify the location of SA and PFAs, and determine the hydraulic flow patterns in CWs annually, except for winter.

The influence of design and operation parameters on flow pattern of CWs

To help to optimize the hydraulic characteristics of CW, correlation analysis was conducted between the $\delta^{18}O$ distribution and design parameter of different CW.

Effect of inflow and outflow types on flow pattern

Water distribution channel was applied in Xiaomei rive CW to guarantee the good distribution of influent. And it can be seen from Fig. 4, there was no obvious SA or PFA around the inlet area throughout the year, except for autumn. In autumn, SA was observed in the east of the inflow channel, which was attributed to the withered reeds. Differed from the Xiaomei river CW, over-fall weirs were adopted in Tuhai river CW. In spring and summer, SAs were gathered on the west side of the inflow channel, while PFAs occurred on the east side near inflow channel (Fig. 4). In autumn and winter, there was no significant difference in $\delta^{18}O$ values that appeared around the over-fall weirs. This phenomenon was attributed to the manual removal of macrophytes in Tuhai river CW after summer. Thus, both inflow types were competent to achieve a uniform and stable water flow, and the SA around the inlet area was likely caused by other factors, i.e., aquatic plants.

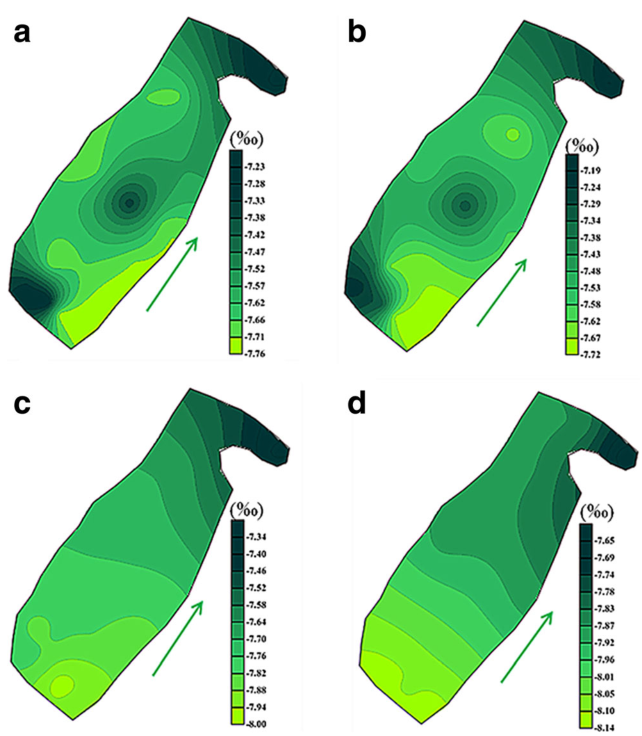

Fig. 4 The isotopes $\delta^{18}O$ distribution of Tuhai river CW in spring (**a**), summer (**b**), autumn (**c**), and winter (**d**). (Arrows represent the direction of water flow)

Outlet ditch which means unilateral overflow was adopted in Xiaomei river CW and was constructed in its southwest corner. The lowest water level on the southwest corner led to a problem that the water flow on the west side had a stronger preferential pathway than that on the east side, resulting in a clear flow stratification. Consequently, the apparent boundary between SAs and PFAs was yielded, and SAs were located on the east side, while PFAs on the west side. The difference in topography was considered an alternative factor for this trend superficially. However, it was no doubt that unilateral overflow aggravated the occurrence of this phenomenon. In Tuhai river CW, over-fall weirs was adopted by the construction of braiding channel. The equal length of flow paths from each cross-section to outlet, due to the lowest water level in the whole outflow cross-section, was beneficial to ensure the stability of outflow in Tuhai river CWs. However, compared with Xiaomei river CW, relatively serious stagnant flow phenomenon was obtained, mainly attributed to the construction of the artificial island in Tuhai river CWs. Thus, over-fall weirs seem to be a better choice than unilateral overflow.

Effect of the plant on flow pattern

Large stretches of macrophytes, either submerged or emergent plants, could increase the flow resistance and change the flow characteristic in CWs. The previous study demonstrated that the flow resistance relied not only on the species of vegetation but also on the density of plant beds (Pham et al. 2011). In the present study, the mixture of submerged plants and emergent plants was introduced into Xiaomei river CW, while Tuhai river CW was dominated by emergent plants (*Zizania aquatica*).

In Xiaomei river CW, SAs were located at E 116° 3′ 30.6″ W 36° 27′ 50.00″, where *reed* and *Vallisneria asiatica* were planted with the density of 277 plants m^{-2}, while the adjacent area was only covered by *reed* with the density of 74 plants m^{-2}. Either submerged plant or emergent plant could produce flow resistance, although dissimilar resistance intensity appeared with the different plant species in the same flow direction (Aberle and Jarvela 2013). As a consequence, the water flow would have priority to pass the areas with smaller flow

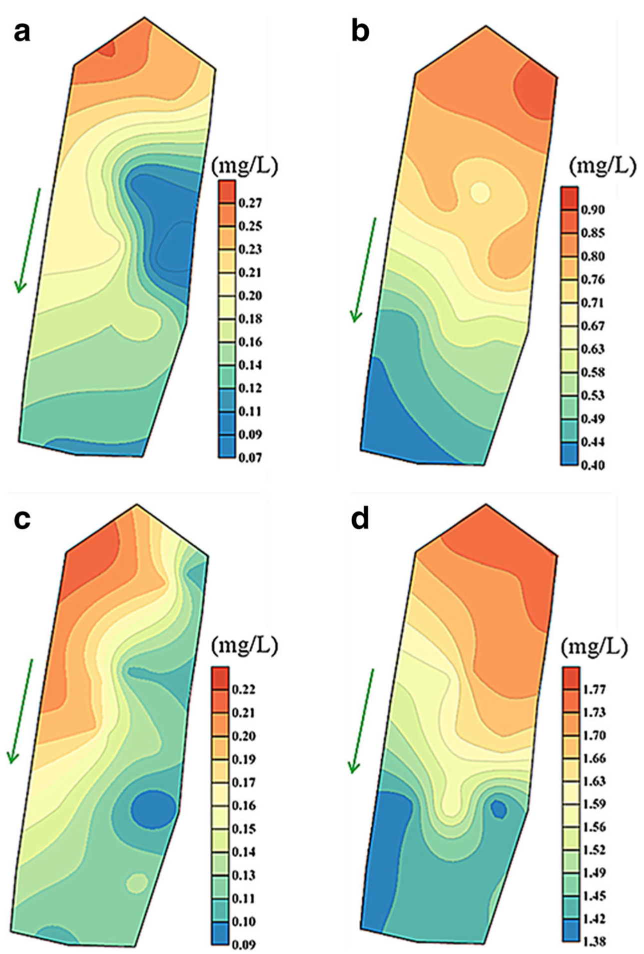

Fig. 5 The ammonia nitrogen distribution of Xiaomei river CW in spring (**a**), summer (**b**), autumn (**c**), and winter (**d**). (Arrows represent the direction of water flow)

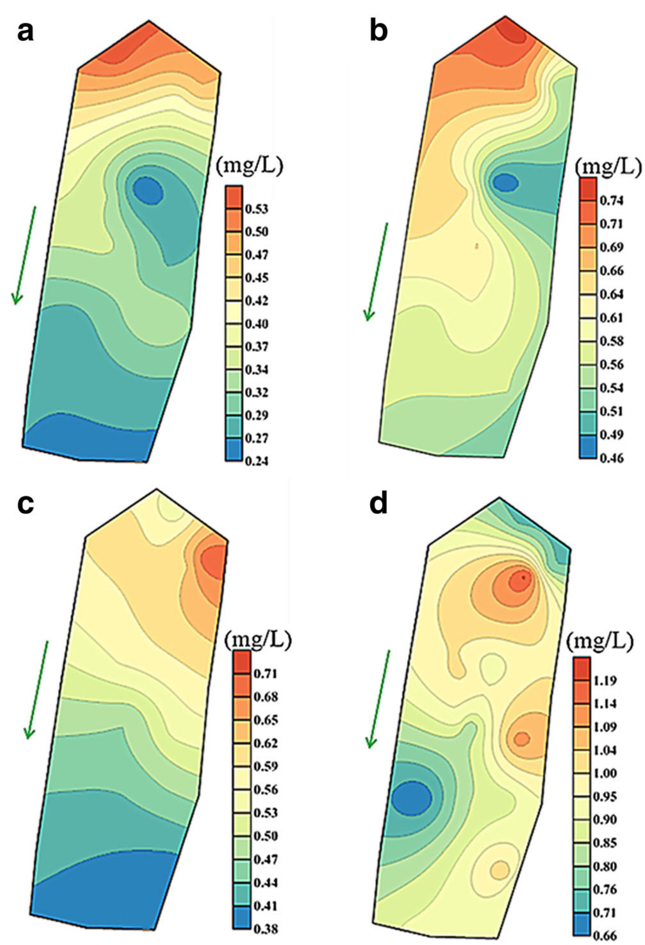

Fig. 6 The TP distribution of Xiaomei river CW in spring (**a**), summer (**b**), autumn (**c**), and winter (**d**). (Arrows represent the direction of water flow)

resistance; meanwhile, extensive SAs were produced in large resistance areas (Ferguson 2012). Stagnant flow phenomenon faded along with the harvest of *reed*, as well as the withered of *Vallisneria asiatica* in winter, which also explained the disappearance of SAs in Fig. 4d.

In addition, plant density was also a major factor influencing flow patterns in CW (Cui et al. 2012; Hua et al. 2014). In Tuhai river CW, stagnant flow appeared in the west of the over-flow weir and the central location of wetland in spring and summer, which were mainly attributed to the difference of plant density. In SAs of Tuhai river CW, plant density of 211 plants m^{-2} and 174 plants m^{-2} were observed, separately, which was higher than other areas. The resistance toward water flow increased with the plant density, due to the energy loss caused by the interaction between water flow and plant (Ruggiero et al. 2003). Stagnant flow disappeared as a consequence of *Zizania aquatic* harvest in autumn. In general, plants played a very important role in hydraulic flow patterns of CW and need careful consideration during its design to prevent negative hydraulic flow patterns.

Annual evaluation of pollutants removal and distribution

Ammonia nitrogen removal and distribution

In Xiaomei river CW, the ammonia nitrogen removal efficiencies were 57.1%, 54.9%, 47.6%, and 18.3% with the influent concentration of 0.28, 0.91, 0.21, and 1.74 mg/L in spring, summer, autumn, and winter, respectively. The high concentration of ammonia nitrogen in CW influent (in other words, effluent of local WWTP) in summer was caused by increasing water consumption and discharge of residents. And in winter, decreased treatment efficiency of WWTP under low temperature was the main reason for the high ammonia nitrogen concertation of its effluent. Low temperature also led to the low ammonia nitrogen removal efficiency (18.3%) of Xiaomei river CW in winter.

Distribution of ammonia nitrogen of Xiaomei river CW in different seasons is illustrated in Fig. 5. It can be seen that the ammonia nitrogen concentration did not decrease along with the flow direction. Instead, some distinct differences at the same transect existed, which was explained by different hydraulic retention time, as well as the differences of plant and microorganism effect in different flow paths (Stottmeister et al. 2003; Toet et al. 2005). In spring and autumn, the ammonia nitrogen concentration in SAs was even less than that in the CW effluent. This distribution property was compatible with those of peatlands in Northern Finland (Ronkanen and Klove 2008). Hydraulic retention time had a significant impact on ammonia removal in CWs, and longer HRT gave arise to maximize nitrification and plant adsorption (Chen et al. 2006). In addition, it was difficult to exchange water between SAs and other areas, which prevented the flow in water with higher ammonia nitrogen concentration (Fan et al. 2016; Stein and Hook 2005).

Total phosphorus removal and distribution

The Xiaomei river CW showed significant seasonal variations in total phosphorus removal efficiency. Total phosphorus removal efficiencies were 57.1%, 40.2%, and 48.6% in spring, summer, and autumn, respectively, while no phosphorus removal was observed in winter. In the present study, the ability of phosphorus adsorption by substrate reaches saturated since Xiaomei river constructed wetland had been operated for six years, and plant adsorption was considered to be the main pathway of phosphorus removal.

As can be seen from Fig. 6, the peak of TP concentration occurred in the inlet area, similar to that of the ammonia nitrogen. In spring and summer, the minimum phosphorus concentration was found in SAs, due to the optimization of efficiency (vigorous macrophyte and active microorganism) in CWs. In autumn, phosphorus concentration decreased along with flow direction. The SAs located in the eastern of water distribution drain showed highest phosphorus concentration, which was attributed to the phosphorus release by lodging plants and decayed leaves and stems (Cheesman et al. 2010; Doig et al. 2017). The distribution of total phosphorus in winter was quite irregular, compared with the other three seasons. And more interestingly, TP concentration in most areas of CW was higher than that in the influent, which was 0.90 mg/L. And the maximum phosphorus concentration in CW could even reach 1.23 mg/L. This could be explained by phosphate desorption from the substrate of CW (Xiang and Zhou 2011). And the relatively low TP concentration in the SAs was mainly relying on the existence of *Potamogenton crispus*, which maintains alive in winter and has been reported to have a considerable effect on phosphorus removal (Wang et al. 2010; Zhang et al. 2015). In general, hydraulic characteristics have a different impact on nitrogen and phosphorus in CW, and the optimization of hydraulic flow patterns in CW should consider its impact on contaminant removal.

Conclusions

In the present study, stable hydrogen and oxygen isotope were introduced to explore the hydraulic flow patterns of field-scale CW. The results of the whole year's measurements showed that stable isotopes of oxygen and hydrogen could be used to determine the hydraulic flow patterns of CW, except for winter when the evaporation was low. Both ammonia nitrogen and total phosphorus distribution were associated with flow patterns. SAs showed better ammonia nitrogen removal performance, while its effect on total phosphorus removal was highly dependent on seasons. Phosphorus release, rather than removal, was observed in winter. Finally, aquatic plants played a significant role in regulating the hydraulic flow pattern of CW and should be well considered during the design of CW.

Funding information This work was supported by the National Natural Science Foundation of China (No. 51878388), Natural Science Foundation of Shandong Province (No. ZR2018QEE006), Shandong Provincial Key Research and Development Program (Major Scientific and Technological Innovation Project) (No. 2019JZZY010411), and Future Plan for Young Scholar of Shandong University.

References

Aberle J, Jarvela J (2013) Flow resistance of emergent rigid and flexible floodplain vegetation. J Hydraul Res 51:33–45

APHA (2017) Standard methods for the examination of water and wastewater, 23rd edn. American Public Health Association, Washington DC

Bodin H, Mietto A, Ehde PM, Persson J, Weisner SEB (2012) Tracer behaviour and analysis of hydraulics in experimental free water surface wetlands. Ecol Eng 49:201–211

Bugna GC, Grace JM, Hsieh Y (2020) Sensitivity of using stable water isotopic tracers to study the hydrology of isolated wetlands in North Florida. J Hydrol 580:124321

Cheesman AW, Turner BL, Inglett PW, Reddy KR (2010) Phosphorus transformations during decomposition of wetland macrophytes. Environ Sci Technol 44:9265–9271

Chen TY, Kao CM, Yeh TY, Chien HY, Chao C (2006) Application of a constructed wetland for industrial wastewater treatment: a pilot-scale study. Chemosphere 64:497–502

Cui L, Zhang Y, Zhang M, Li W, Zhao X, Li S, Wang Y (2012) Identification and modelling the HRT distribution in subsurface constructed wetland. J Environ Monit 14:3037–3044

Das S, Mazumdar A (2015) Comparison of kinematics of horseshoe vortex at a flat plate and different shaped piers. Int J Fluid Mech Res 42:418–448

Dayem KE, Molnar P, Battisti DS, Roe GH (2010) Lessons learned from oxygen isotopes in modern precipitation applied to interpretation of speleothem records of paleoclimate from eastern Asia. Earth Planet Sci Lett 295:219–230

Doig LE, North RL, Hudson JJ, Hewlett C, Lindenschmidt KE, Liber K (2017) Phosphorus release from sediments in a river-valley reservoir in the northern Great Plains of North America. Hydrobiologia 787: 323–339

Fan J, Zhang J, Huu Hao N, Guo W, Yin X (2016) Improving low-temperature performance of surface flow constructed wetlands using *Potamogeton crispus* L. plant. Bioresour Technol 218:1257–1260

Ferguson RI (2012) River channel slope, flow resistance, and gravel entrainment thresholds. Water Resour Res 48:W05517

Gooddy DC, Lapworth DJ, Bennett SA, Heaton THE, Williams PJ, Surridge BWJ (2016) A multi-stable isotope framework to understand eutrophication in aquatic ecosystems. Water Res 88:623–633

Guo C, Cui Y, Dong B, Liu F (2017) Tracer study of the hydraulic performance of constructed wetlands planted with three different aquatic plant species. Ecol Eng 102:433–442

Gupta P, Noone D, Galewsky J, Sweeney C, Vaughn BH (2009) A new laser-based, field-deployable analyzer for laboratory-class stable isotope measurements in water. Geochim Cosmochim Acta 73: A480–A480

Hua GF, Zhao ZW, Kong J, Guo R, Zeng YT, Zhao LF, Zhu QD (2014) Effects of plant roots on the hydraulic performance during the clogging process in mesocosm vertical flow constructed wetlands. Environ Sci Pollut Res 21:13017–13026

Kele S, Ozkul M, Forizs I, Gokgoz A, Baykara MO, Alcicek MC, Nemeth T (2011) Stable isotope geochemical study of Pamukkale travertines: new evidences of low-temperature non-equilibrium calcite-water fractionation. Sediment Geol 238:191–212

Laurent J, Bois P, Nuel M, Wanko A (2015) Systemic models of full-scale surface flow treatment wetlands: determination by application of fluorescent tracers. Chem Eng J 264:389–398

Lécuyer C, Amiot R, Touzeau A, Trotter J (2013) Calibration of the phosphate $\delta^{18}O$ thermometer with carbonate–water oxygen isotope fractionation equations. Chem Geol 347:217–226

Lin AY, Debroux J, Cunningham JA, Reinhard M (2003) Comparison of rhodamine WT and bromide in the determination of hydraulic characteristics of constructed wetlands. Ecol Eng 20:75–88

Liu J, Dong B, Zhou W, Qian Z (2020) Optimal selection of hydraulic indexes with classical test theory to compare hydraulic performance of constructed wetlands. Ecol Eng 143:105687

Min J, Wise WR (2009) Simulating short-circuiting flow in a constructed wetland: the implications of bathymetry and vegetation effects. Hydrol Process 23:830–841

Muste M, Vermeyen T, Hotchkiss R, Oberg K (2007) Acoustic velocimetry for riverine environments. Hydraul Eng 133:1297–1298

Nyantekyi-Kwakye B, Tachie MF, Clark SP, Malenchak J, Muluye GY (2017) Acoustic Doppler velocimeter measurements of a submerged three-dimensional offset jet flow over rough surfaces. J Hydraul Res 55:40–49

Pham N, Penning E, Mynett A, Raghuraj R (2011) Effects of submerged tropical macrophytes on flow resistance and velocity profiles in open channels. Int J River Basin Manag 9:195–203

Plugatyr A, Svishchev IM (2008) Residence time distribution measurements and flow modeling in a supercritical water oxidation reactor: application of transfer function concept. J Supercrit Fluids 44:31–39

Pugliese L, Kusk M, Iversen BV, Kjaergaard C (2020) Internal hydraulics and wind effect in a surface flow constructed wetland receiving agricultural drainage water. Ecol Eng 144:105661

Qi W, Guo Y, Xue M, Li Y (2013) Hydraulic analysis of an upflow sand filter: tracer experiments, mathematical model and CFD computation. Chem Eng Sci 104:460–472

Ronkanen A, Klove B (2007) Use of stabile isotopes and tracers to detect preferential flow patterns in a peatland treating municipal wastewater. J Hydrol 347:418–429

Ronkanen A, Klove B (2008) Hydraulics and flow modelling of water treatment wetlands constructed on peatlands in Northern Finland. Water Res 42:4894–4894

Ruggiero C, De Pascale S, Angelino G, Maggio A (2003) Developmental changes in plant resistance to water flow in Pisum sativum (L.). Plant Soil 250:121–128

State Environmental Protection Administration (2002) Water and wastewater monitoring analysis method, 4th edn. China Environmental Science Press, Beijing

Stein OR, Hook PB (2005) Temperature, plants, and oxygen: how does season affect constructed wetland performance? J Environ Sci Health A 40:1331–1342

Stottmeister U, Wiessner A, Kuschk P, Kappelmeyer U, Kastner M, Bederski O, Muller RA, Moormann H (2003) Effects of plants and microorganisms in constructed wetlands for wastewater treatment. Biotechnol Adv 22:93–117

Sun H, Hu Z, Zhang J, Wu W, Liang S, Lu S, Liu H (2016) Determination of hydraulic flow patterns in constructed wetlands using hydrogen and oxygen isotopes. J Mol Liq 223:775–780

Tang P, Yu B, Zhou Y, Zhang Y, Li J (2017) Clogging development and hydraulic performance of the horizontal subsurface flow stormwater constructed wetlands: a laboratory study. Environ Sci Pollut Res 24: 9210–9219

Toet S, Van Logtestijn RSP, Kampf R, Schreijer M, Verhoeven JTA (2005) The effect of hydraulic retention time on the removal of pollutants from sewage treatment plant effluent in a surface-flow wetland system. Wetlands 25:375–391

Vymazal J (2007) Removal of nutrients in various types of constructed wetlands. Sci Total Environ 380:48–65

Vymazal J (2010) Constructed wetlands for wastewater treatment: five decades of experience. C R C Crit Rev Environ Control 31:351–409

Vymazal J (2011) Constructed wetlands for wastewater treatment: five decades of experience. Environ Sci Technol 45:61–69

Wang L, Wang G, Yu Z, Gu X, Chen Q (2010) Effect of submerged plant *Potamogeton crispus* on the concentrations of phosphorus fractions in overlying water, 2010 IEEE 2nd Symposium on Web Society (SWS 2010). IEEE, Beijing, China, pp 197–200

Woodard R (2000) Interpolation of spatial data: some theory for Kriging. Technometrics 42:436–437

Xiang S, Zhou W (2011) Phosphorus forms and distribution in the sediments of Poyang Lake, China. Int J Sediment Res 26:230–238

Yu J, Yu F, Liu D (1987) Hydrogen and oxygen isotopic compositions of meteoric waters in the eastern part of China. Chin J Geochem 6:367–371

Zhang Y, He F, Xia S, Zhou Q, Wu Z (2015) Studies on the treatment efficiency of sediment phosphorus with a combined technology of PCFM and submerged macrophytes. Environ Pollut 206:705–711

Zheng L, Ding AZ, Kong DC, Cheng LR (2011) Hydraulic characteristics of a pilot-scale vertical subsurface flow constructed wetland, International Conference on Energy, Environment and Sustainable Development (ICEESD 2011). Advanced Materials Research, Shanghai Univ Elect Power, Shanghai, PEOPLES R CHINA, pp 2451–2458